Solar-Terrestrial Physics. 2023. Vol. 9. Iss. 4. P. 37–45. DOI: 10.12737/stp-94202305. © 2023 A.V. Borovik, A.A. Zhdanov. Published by INFRA-M Academic Publishing House

UDC 523.98
DOI: 10.12737/stp-94202305

Received September 02, 2023
Accepted November 09, 2023

DYNAMICS OF SMALL-SCALE MAGNETIC FIELDS BEFORE SMALL AND LARGE SOLAR FLARES

A.V. Borovik
Institute of Solar-Terrestrial Physics SB RAS, Irkutsk, Russia, aborovik@iszf.irk.ru

A.A. Zhdanov
Institute of Solar-Terrestrial Physics SB RAS, Irkutsk, Russia, azhdanov@iszf.irk.ru

Abstract. We have examined the dynamics of the longitudinal magnetic field of active region NOAA 12673, using data from the Solar Dynamics Observatory (SDO). During the passage of the active region (AR) across the solar disk, its spots and background fields showed complex motion trajectories, and numerous small-scale short-lived local polarity inversion lines (LPILs) were formed when new magnetic fluxes appeared in the AR and came closer to fields of opposite polarity. The length of LPILs was less than 15.000 km (~20 arcsec); their lifetime was several hours. Study of the flare activity of NOAA 12673 has shown that low-power flares (optical class S, area <2 sq. degrees) generally occur near LPILs. Before small flares and the September 06, 2017 large flare (optical importance 3B, X-ray class X9.3), in limited sites of local and main polarity inversion lines there were shear stresses and an increase in the magnetic field gradient: in the region of low-power flares, to 1.3–1.5 G/km; in the region of the large flare, 3–3.5 G/km. The results obtained suggest that the longitudinal magnetic field behaves similarly before both small and large flares.

Keywords: flares, magnetic fields, polarity inversion lines.

INTRODUCTION

One of the fundamental questions in solar-terrestrial physics is the question concerning the mechanisms of energy accumulation by solar flares. It is believed that the source is the free magnetic field energy excess with respect to the energy of the potential field of sunspots and background magnetic fields. The accumulation of free energy on the Sun in active regions (ARs) is caused by the rotation of sunspots, vortex and shear solar plasma flows (magnetic field shear) [Hagyard et al., 1984]; in quiet regions, by the rotation of plages [Sundara et al., 1997; Cao et al., 1983]. There are many theoretical schemes explaining the nature of solar flares and individual flare phenomena. The energy accumulated by a magnetic field is assumed to be released when a new magnetic flux from under the photosphere penetrates into coronal magnetic fields of ARs [Krivsky, 1968]. At the region of interaction of the emerging opposite polarity flux with old magnetic fields, current sheets are formed. Over time, due to a number of instabilities, current systems are disrupted, followed by rapid magnetic field line reconnection and free magnetic field energy release in the form of a flare. It is claimed that the flare type is determined by the magnetic environment into which the flux penetrates [Heyvaerts et al., 1977]. If a new flux emerges near the AR filament close to the polarity inversion line (PIL), this leads to the formation of a two-ribbon flare of optical class ≥2 with 10^{32}–10^{33} erg energy. According to the currently dominant CSHKP model that combines different observational and theoretical schemes, upon flux penetration a filament (plasmoid) becomes unstable when field lines curve and is ejected upwards. This leads to the compression of solar plasma surrounding PIL and to the formation of a current sheet, followed by magnetic field line reconnection and free energy release in the overlying magnetic field [McKenzie, 2002]. There are three main forms of energy release: hydrodynamic motions (current sheet disruption accompanied by rapid plasma motions), thermal heating (high-power heat fluxes) in the region of the current sheet disruption, and the flux of a large number (up to 10^{38}) of high-energy electrons and ions with energy from 20 keV to several tens of MeV. Due to thermal conductivity and non-thermal particles freely propagating along magnetic loops, the energy spreads into the chromosphere [Hoyng et al., 1981], heats chromospheric plasma to tens of millions of degrees, causes its evaporation, and gives rise to double sources of hard X-rays and flare ribbons in the Hα line. It has to be said that solar flares actually are not as symmetrical as in model schemes, and there are many observations that do not fit into models. In this regard, the study and analysis of flare events are still relevant today.

Large powerful flares usually occur at solar maximum and during the decline phase of solar activity with several flares per year. They generate a complex chain of dynamic processes in the solar atmosphere, have an effect on the radiation situation in near space, Earth's magnetosphere, ionosphere, and neutral atmosphere, affect the operation of spacecraft, communication and navigation systems. Powerful flares have therefore aroused increasing interest among researchers all the time. Although the mechanisms of their generation have not yet been fully understood, at present there is a virtually complete body of knowledge about such flares [Svestka, 1976; Altyntsev et al., 1982].

At the same time, there are many low-power solar flares both in active and quiet regions. We classify flares with an area of <2 sq. deg and an energy of ~10^{29} erg in the Hα line as small flares (SFs). During some periods, the rate of their occurrence may be as high as 1 flare per 5 min. At this time, it is difficult to distinguish SF from the boiling of a plage. That is why, many researches consider SFs as background events and do not record them. For this or other reasons, no systematic comprehensive study of SFs has been undertaken to date. Small flares are believed to represent a simple loop-type structure. In soft X-rays, they have short time scales, small volumes, low heights, high energy densities. Energy is usually released during the impulsive phase. Typically there is a single hard X-ray burst lasting for about one minute. In [Heyvaerts et al., 1977; Priest, 1985], it is stated that SFs occur when a new magnetic flux emerges near unipolar sunspots at the edge of AR or around its unipolar fields. The interaction of the flux with the overlying magnetic field yields a current sheet, in turbulent plasma of which magnetic fields rapidly reconnect followed by mass ejections (serge) and a particle flux, which cause SFs in Hα in the lower chromosphere. In the 1980s, their research actually stopped. Since the beginning of spacecraft flights, the main attention has been paid to the theory of heating the solar corona by nanoflares [Parker, 1988]. Meanwhile, the results of early studies on SFs suggest that while significantly differing in power and area in the Hα line, they may show scenarios similar to large flares [Altyntsev et al., 1982]. In support of this, in [Borovik, Zhdanov, 2018] from extensive statistical material (more than 80 thousand flares) it has been found that in terms of features of SF development they do not differ from large flares: they are accompanied by activation and disappearance of filaments, occur near PILs, have an explosive phase and multiple bursts of intensity. Among them are flares covering sunspot umbra, two-ribbon and white flares. Using data on solar cycles 21–24, Borovik et al. [2020] have also shown that SFs are grouped in the regions where magnetic fluxes emerge at an intensive rate mainly in the tail and central parts of sunspot groups. Like large energetic flares, SFs can be accompanied by proton fluxes and X-rays of different power, including X class [Borovik, Zhdanov, 2020]. These facts suggest that the nature and mechanisms of SF occurrence are of great significance for the research aiming at understanding the development of the flare process in its relatively simple manifestation and clarifying whether there is a single physical mechanism underlying the flares of different power or these flares differ in nature.

In recent decades, observations of the solar atmosphere at high spatial and temporal resolution have become possible with the help of spacecraft. This made it possible to study small flares at a higher quality level. This paper presents the results of a study of flare activity of sunspot group NOAA 12673 based on observational data from the Solar Dynamics Observatory (SDO) (Figure 1). The active region was distinguished for its complex structure and high dynamics of magnetic fields [Yang et al., 2017; Verma, 2018; Romano et al., 2019]. When passing across the solar disk, the AR exhibited massive emergence of arched filament systems (AFS) without large filaments. In September 2017, it produced a series of powerful flares and an X9.3-class X-ray flare, the largest in the past decade.

1. DATA

We have employed SDO/HMI and AIA observations [http://jsoc.stanford.edu]. The dynamics of the longitudinal magnetic field in AR was studied from full solar disk HMI magnetograms (0.5″ px^{-1} angular resolution; 45 s^{-1} frame rate). The photosphere was analyzed from HMI-continuum images. To identify flares in the solar corona, we have used SDO/AIA solar images in the 171 Å line and GONG observations in the Hα line [https://gong.nso.edu].

2. RESULTS

2.1. Dynamics of magnetic fields in active region NOAA 12673

When AR passed across the solar disk, its spots and magnetic fields of different scales rotated and moved unevenly along complex trajectories (Figure 2). Panel *a* shows motions of small-scale fields and sunspots on September 3, 2017. Background fields >80 G are indicated by the color of the corresponding polarity. Large arrows are paths of sunspots (contours are outlined with a dashed line); small arrows, paths of small-scale fields. The dashed line marks LPILs I and II. Yellow arrows denote locations of three small flares f1, f2, and f3 (Section 2.2).

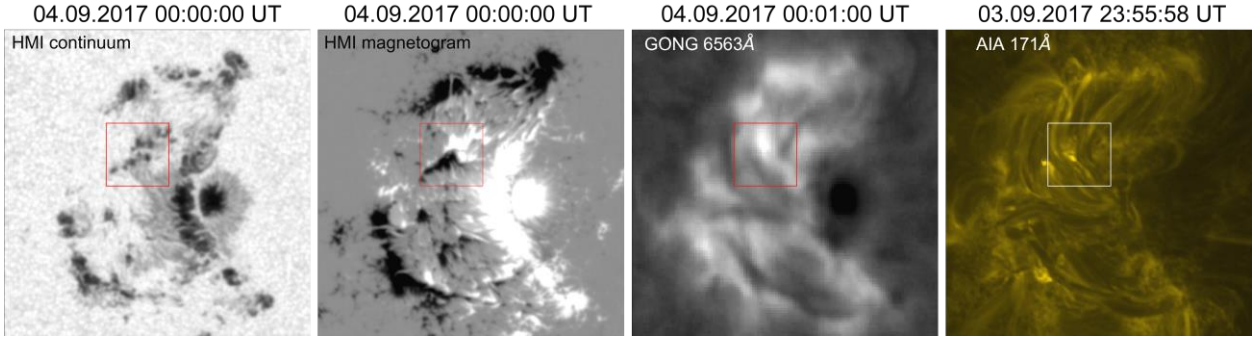

Figure 1. Active region NOAA 12673 as observed in the continuum (SDO/HMI), in the Hα (GONG) and 171 Å (SDO/AIA) lines. An HMI magnetogram of AR is given. The SF region is marked with a 25×25 px square

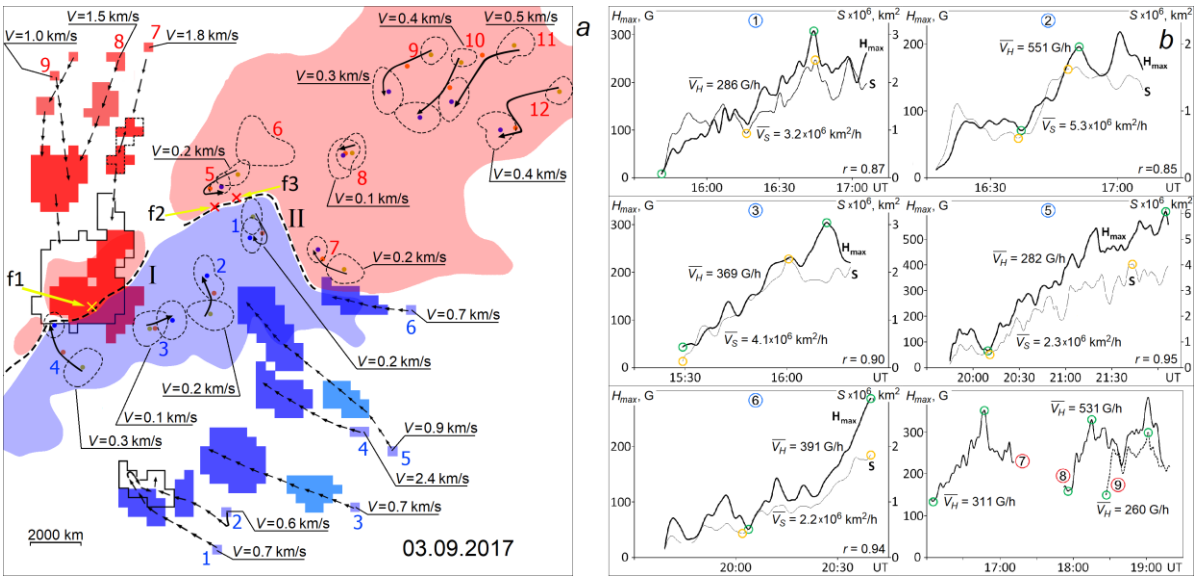

Figure 2. Dynamics of magnetic fields of NOAA 12673. Arrows denote motions of small-scale magnetic fluxes (1-6 and 7-9) and sunspots (1-4 and 5-12) (*a*); changes in the area and maximum intensity of small-scale magnetic fluxes (*b*)

Average velocities of the sunspots were 0.1–0.5 km/s, which is comparable to the velocities of horizontal plasma flows in convection cells (0.3–0.5 km/s). With the appearance of small-scale multipolar fluxes in the AR (1-6, 7-9), they moved at an uneven velocity from 0.1 to 0.7 km/s towards large-scale background fields of the same polarity until they completely merged with them. In some cases, the average velocities were 1–2.4 km/s. The moving small-scale fluxes were also observed to merge (see Figure 2). The regions formed as a result of the coalescence of unipolar small-scale fields are highlighted with a solid line.

As the small-scale fields moved, their area and maximum intensity increased with time. Rates of the changes were $(2.2 \div 5.3) \cdot 10^6$ km^2/h and 260–550 G/h respectively (panel *b*). At the same time, the correlation coefficients *r* between H_{max} and *S* were high (~0.9 and higher).

This behavior of the emerging magnetic fluxes resembles the Piddington model [Piddington, 1975], which assumes that in the sub-photospheric layer the toroidal field is a tree whose trunk is the main magnetic flux rope, and the upper branches are weak large-scale fields and unipolar magnetic regions. Going out into the solar atmosphere, the magnetic flux rope gradually untwists and straightens. As a result, tree branches — small-scale magnetic structures — rise to the surface of the photosphere.

2.2. Local polarity inversion lines of the longitudinal magnetic field

Motions of large-scale and emerging small-scale magnetic fields and their convergence with the fields of opposite polarity led to the formation of numerous local short-lived small-scale PILs (LPILs) in the active region (Figures 2, 3). For better clarity, the SDO/HMI magnetograms are shown in color of the corresponding polarity: red — S, blue — N.

The lifetime of LPILs was several hours; their length was less than 15000 km (20 arcsec). For comparison: the main PIL (see Figure 15) formed before large flares on September 6, 2017 for two days and existed for four days before its complete decay. Its length was ~60000 km (~80 arcsec), i.e. LPILs are more than four times shorter than PILs, and their lifetime is ten times shorter.

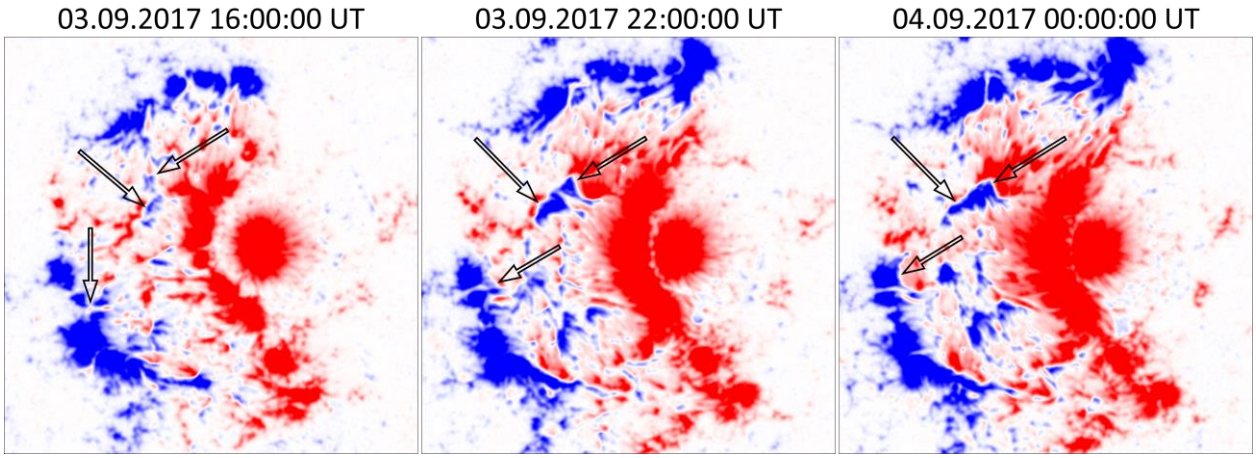

Figure 3. Local polarity inversion lines of the longitudinal magnetic field of AR NOAA 12673 (S10W03). Blue and red colors are the fields of N and S polarities. Arrows show three regions of LPIL formation

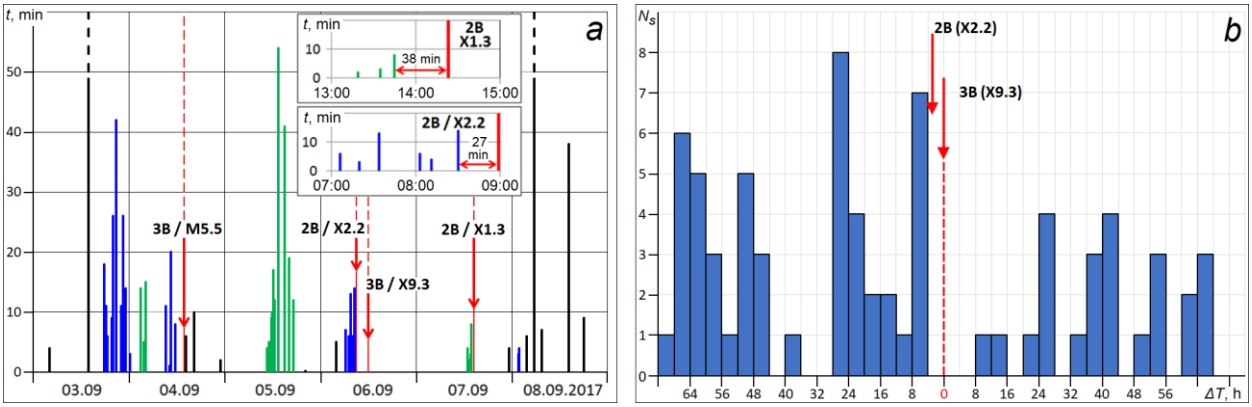

Figure 4. Flare activity of NOAA 12673 (September 3–8, 2017)

2.3. Solar flares

Active region NOAA 12673 was characterized by high flare activity. In addition to three powerful X-class flares, there were 84 SFs recorded in the AR, including 11 on September 3 and 8 on September 6 (Figure 4). In panel *a*, the SF series are highlighted in different colors (*t* is the duration of the flares). The time sequence of SFs before two powerful flares is scaled up.

Panel *b* presents a histogram of the number of SFs at 4 hr intervals relative to the beginning of the X9.3 class flare (September 06, 2017, 11:54 UT).

Note that before large energetic flares the number of SFs decreases. This confirms the conclusions made in [Borovik, 2023] about the absence or weak SF activity before large flares.

In total, we have analyzed nine SFs and one energetic two-ribbon flare occurring on September 06, 2017 (3B optical importance, X9.3 X-ray class).

September 03, 2017 low-power flare (f1)

The flare occurred at 23:31:30 UT near LPIL I (see Figure 5; Figure 6 (black arrow)) and lasted for ~3 min. Figure 6 (as well as Figures 10, 13, 15) illustrates changes in the magnetic field structure in the flare region. On the color scale are gradations of the magnetic field strength to 750 G.

2.3.1. Low-power flares

Low-power flares occurred near LPIL during motions, coalescence, and extension of sunspots (Figure 5, yellow arrows). Their fragmentation was also observed. A relationship between SF and LPIL has also been established for three SFs in AR NOAA 12674 (N14E13), developing north of NOAA 12673. The presence of secondary PILs in AR (in addition to the main one) is mentioned in the monograph [Altyntsev et al., 1982]. Their existence has been confirmed by Borovik [1994]; the author shows that there is a relationship between secondary PILs and centers of SF activity.

Motions of magnetic fields near LPIL led to its displacement, deformation, and rotation around a certain center (Figure 7, *a* (arrow)). Velocities of the displacement of LPIL at different sections were different, comparable in some cases with the velocity of horizontal plasma flows in convection cells.

We have analyzed variations in the magnetic field strength and gradient along LPIL. To do this, at the onset of the flare, the LPIL was divided into sections in perpendicular segments of 2 arcsec with a step of 1 px (see Figure 6). Then, the segments were transferred to subsequent and previous magnetograms; field strengths and gradients were determined at the endpoints. We have processed 161 magnetograms. The study was limited to a two-hour interval — an hour before and an hour after the flare. Variations in *H* and grad*H* smoothed by a Savitsky—Goley filter are plotted in Figures 8, 9.

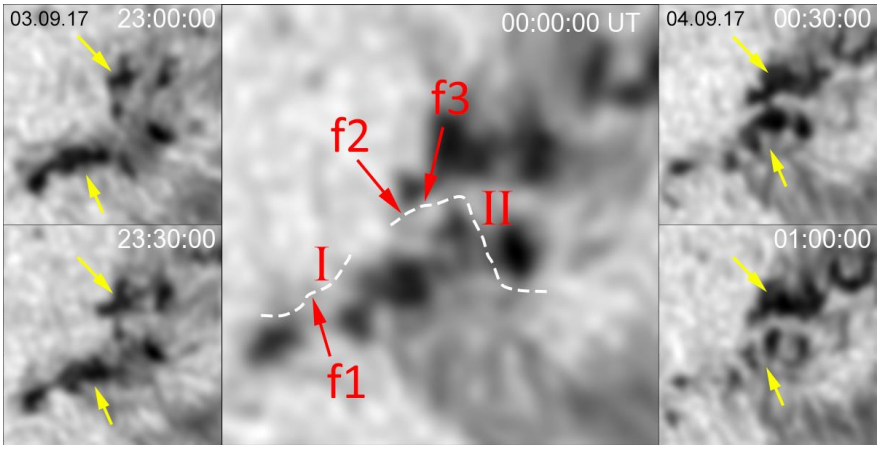

Figure 5. Activity of sunspots near LPILs I and II before and after SF

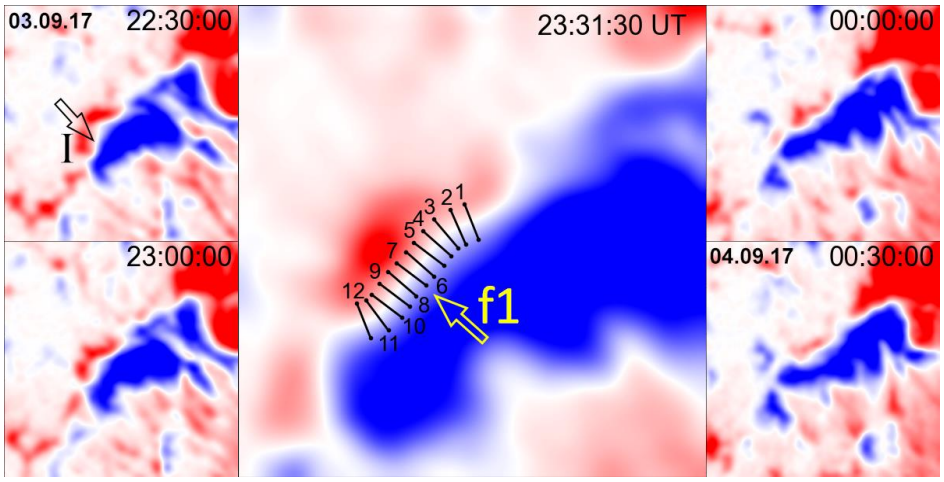

Figure 6. Change in the magnetic field structure in f1 on September 3–4, 2017

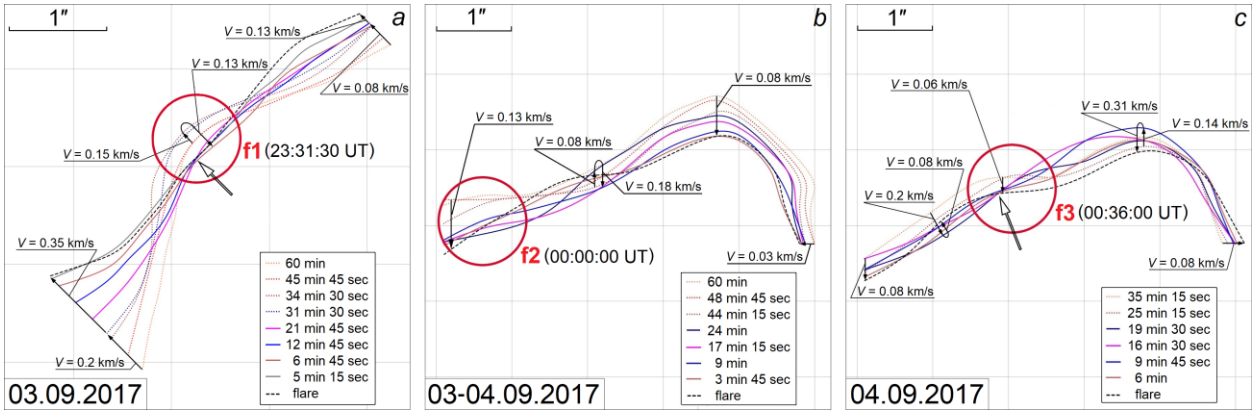

Figure 7. Motions of LPIL before f1, f2, and f3. Red circles mark the flare regions. Colored lines indicate LPIL locations at certain time points (Tables). Black dashed lines denote LPIL locations at the onset of the flare. Arrows show motion directions and average velocities

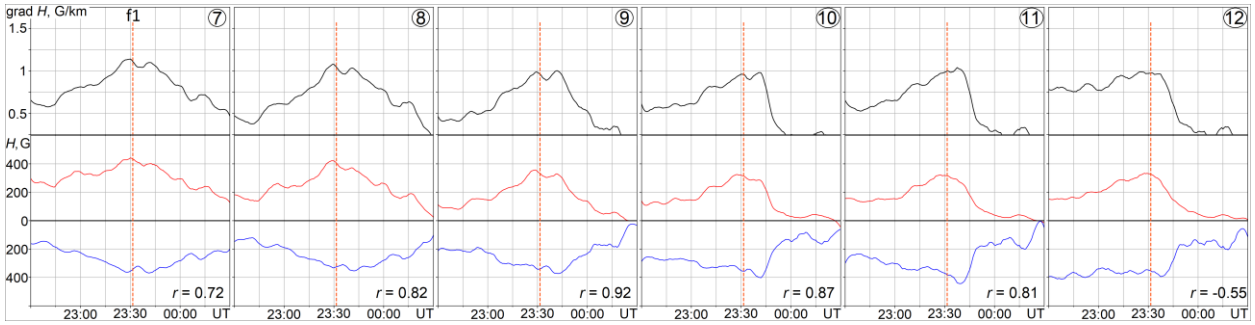

*Figure 8.*Variations in *H* and grad*H* along LPIL in the f1 region . Top panels are grad*H*; bottom panels, *H* (the S-polarity field is shown in red; N, in blue; *r* is the correlation coefficient)

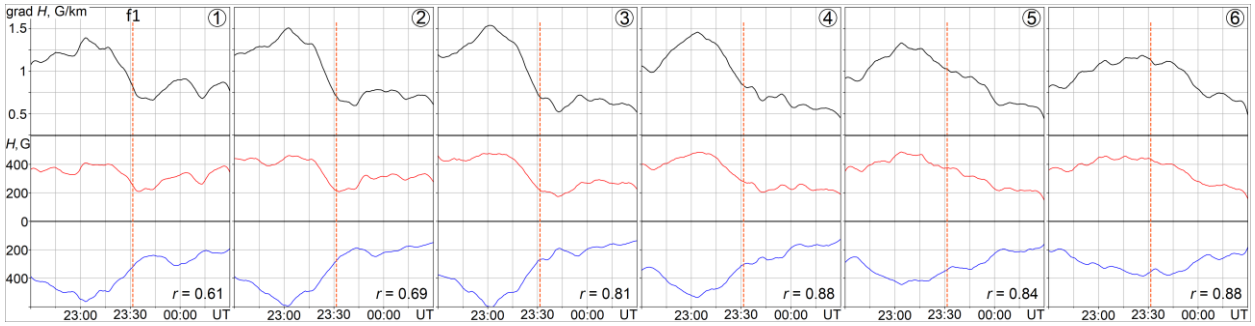

Figure 9. Variations in *H* and grad*H* along LPIL sections 1–6

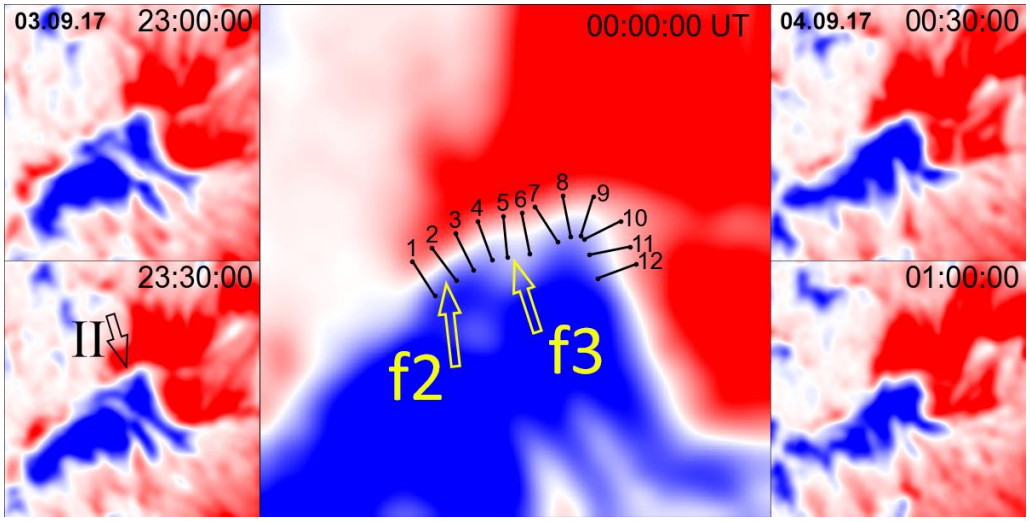

Figure 10. Changes in the magnetic field structure in the f2 and f3 regions on September 3–4, 2017

In the f1 region, an increase in grad*H* was detected in sections 7–12 (see Figure 8). It reached a maximum value of 1.25 G/km at the onset of the flare. Then came a decrease. In other LPIL sections (1–6), a grad*H* growth was weak, decreased, or completely absent (see Figure 9).

September 04, 2017 low-power flares (f2, f3)

The flares occurred near LPIL II (see Figures 5, 10): f2 — at 00:00:10 UT, ~6 min; f3 — near f2 at 00:36:10 UT, ~8 min. Similarly to f1, the pre-flare changes in the magnetic field before f2 caused the LPIL to shift, deform, and rotate around a certain center (see Figure 7, *b*).

It was found that in sections 1–4 in f2, as before f1, there was an increase in grad*H* (Figure 11, *a*). The field also reached a maximum gradient of 1.34 G/km at the onset of the flare. In other sections, grad*H* did not change significantly (see Figure 12, *a*).

The flare f3 occurred 36 min after f2 on the same LPIL at 00:36:10 UT (see Figures 5, 10). As in f1 and f2, variations in grad*H* an hour before the flare (see Figure 11, *b*) show an increase in sections 4–6. The maximum gradient was 1.46 G/km. No such variations were observed in other sections (see Figure 12).

In the regions of the three flares, high (0.9 and higher), direct, and cross correlations were found between fields of opposite polarity (see Figures 8, 9, 11, 12, 13). This suggests that there were coupled bipolar magnetic field structures on opposite sides of the LPIL and shear magnetic field strengths.

From the results obtained it follows that an increase in grad*H* to 1.3–1.5 G/km in restricted LPIL sections 40–90 min before a flare and the presence of shear field strengths in their region are a necessary condition for the occurrence of SFs.

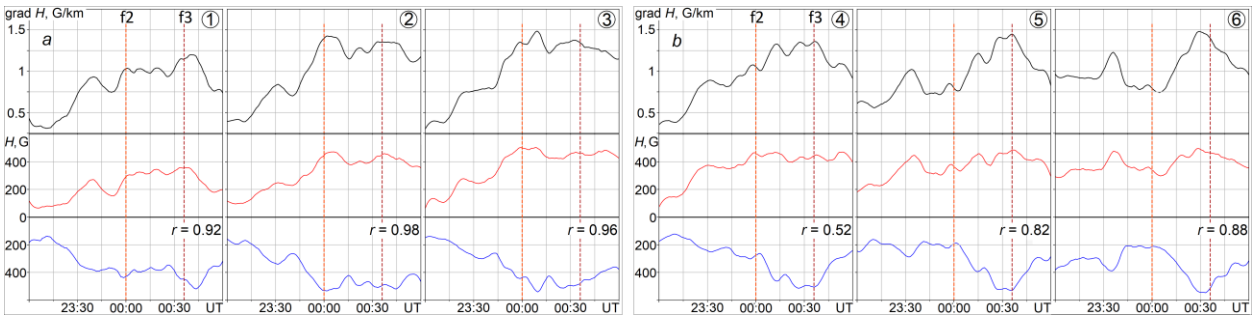

Figure 11. Variations in *H* and grad*H* in f2 (*a*) and f3 (*b*)

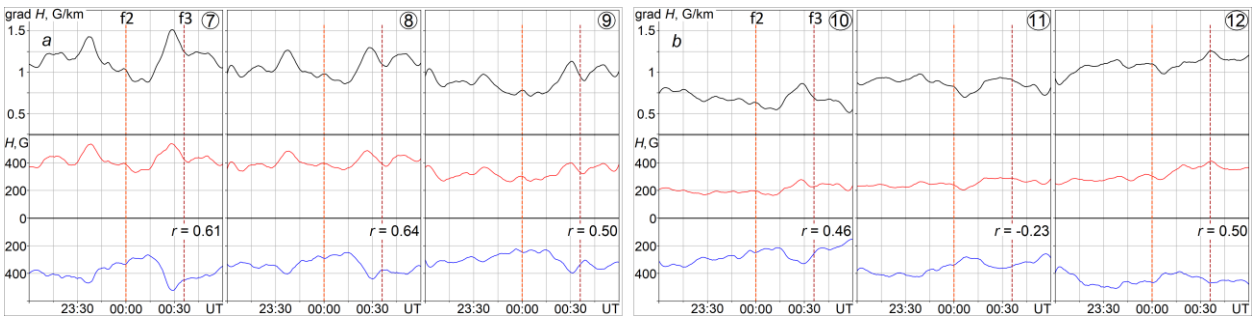

Figure 12. Variations in *H* and grad*H* along LPIL sections 7–12 before f2 and f3

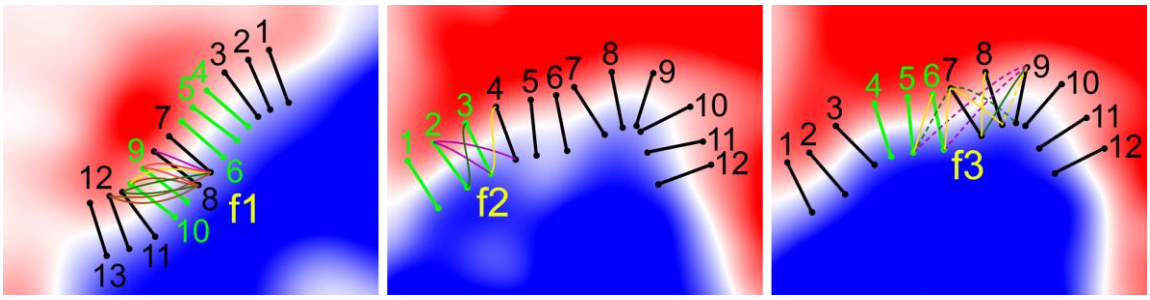

Figure 13. Correlations between magnetic fields of opposite polarity in the SF region. Direct correlations are shown in green. For f1 and f2, the correlation coefficients are 0.9 and higher; for f3: 0.8–0.85 (dashed line), 0.85 and higher (solid line)

2.3.2. September 6, 2017 powerful solar flare

To establish that the phenomena detected in f1, f2, and f3 are typical, a similar study has been carried out for a large two-ribbon flare that occurred in the AR on September 6, 2017 at 11:54 UT. It was found that the X9.3 flare, as well as small flares, was preceded by motions of large-scale magnetic fields, LPIL displacement, deformation, and rotation around a certain center (see Figures 14, 15). It was also established that 103–47 min before the flare grad*H* increased in sections 12–19 of the main PIL, as before SF. By the beginning of the flare, it reached a maximum value 3–3.5 G/km (Figure 16). No such phenomenon was observed in other sections of the PIL (Figure 17).

Direct and cross correlations were detected between the fields of opposite polarity in PIL sections 13–20 (see Figure 15, *b*). In some cases, the correlation coefficient approached 1 (see Figure 16), which suggested that there were shear field strengths in the flare region.

It is noteworthy that all the flares considered were identified in the solar corona as bright loops and knots a few minutes before their onsets (see Figures 1, 14). In the 171 Å line, microflares also occur in the absence of Hα flares. It can be assumed that in such cases the energy of particles accelerated in the coronal source was not enough to cause a full-fledged chromospheric flare.

CONCLUSIONS

1. All the low-power flares we have studied occurred during well-defined dynamics of small-scale magnetic structures of the active region and large-scale field variations.
2. We have found that SFs appeared near small-scale short-lived LPILs formed in AR NOAA 12673 during the emergence of new small-scale magnetic fluxes, their displacement, coalescence, and convergence with fields of opposite polarities.
3. The appearance of SFs is likely to be caused by an increase in the field gradient in certain sections of LPILs to 1.3–1.5 G/km and shear magnetic field strengths occurring in the flare region. According to modern modelling views, the convergence of magnetic fields of opposite polarities on PIL leads to magnetic field reconnection and pulsed free energy release in the form of a flare.

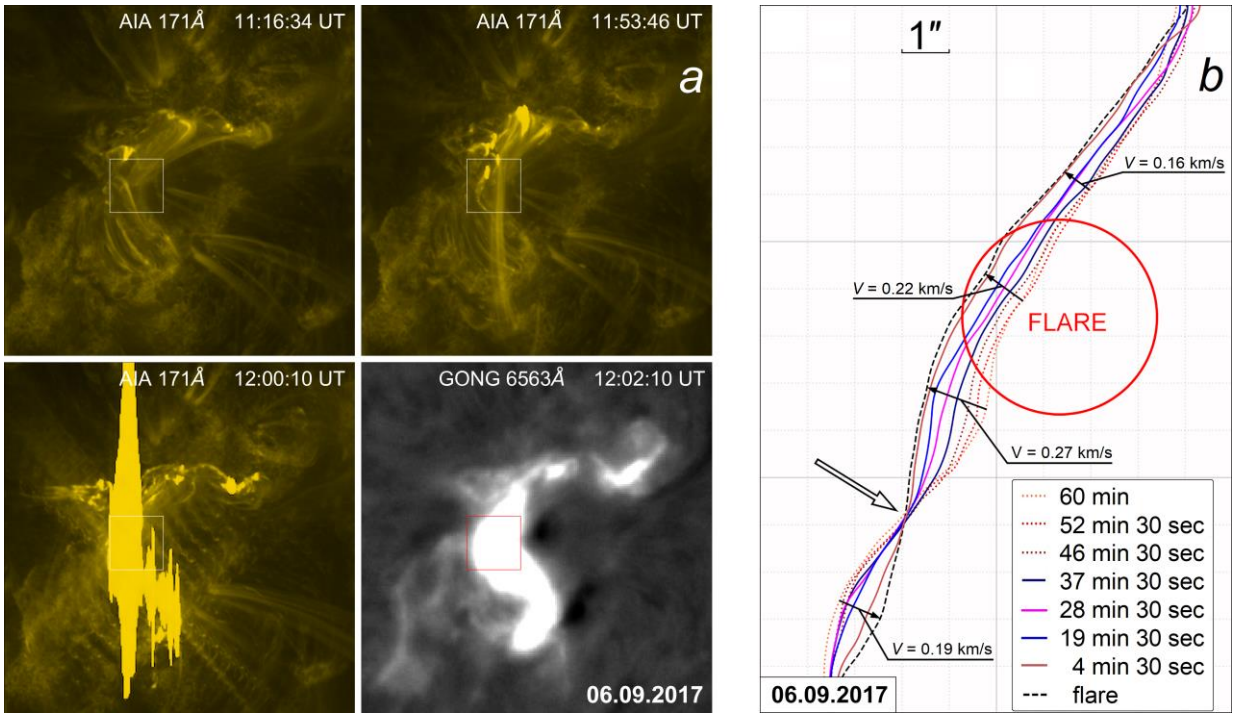

Figure 14. Powerful flare on September 06, 2017 (11:54 UT) in the 171 Å and Hα lines (maximum development) (*a*); PIL motion an hour before the flare (*b*). The red circle marks the part of the flare that was separately observed in the Hα line

4. Analysis of the magnetic field dynamics before the X9.3-class X-ray flare has shown that similar processes occur before large flares. At the same time, the maximum field gradient in a certain PIL section was 3–3.5 G/km. It follows from the results obtained that the mechanisms for the occurrence of solar flares having different areas and power may not differ fundamentally.

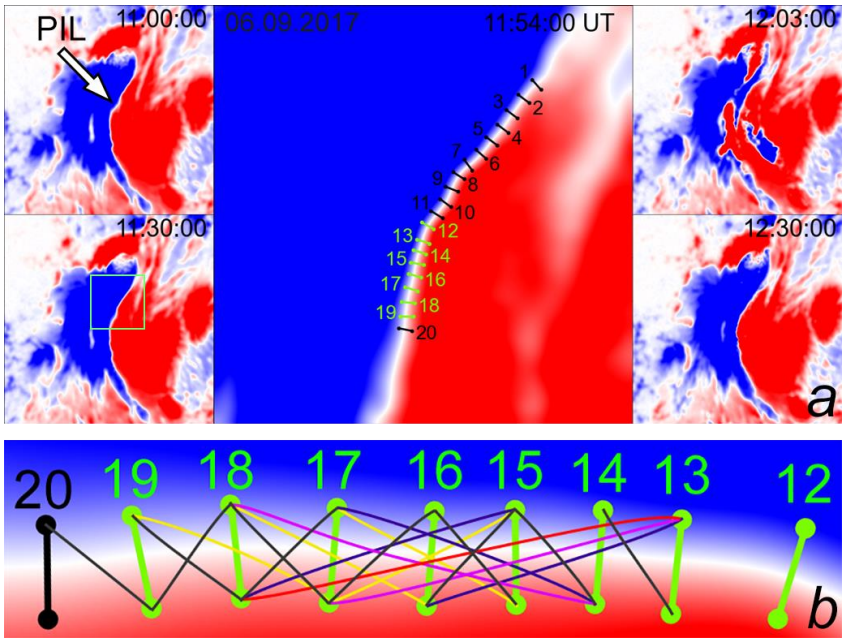

Figure 15. Structure of the AR magnetic field an hour before and an hour after the powerful flare (*a*); correlations in the region of the powerful flare between magnetic fields of opposite polarity (r=0.9 and higher): direct (green) and cross (*b*)

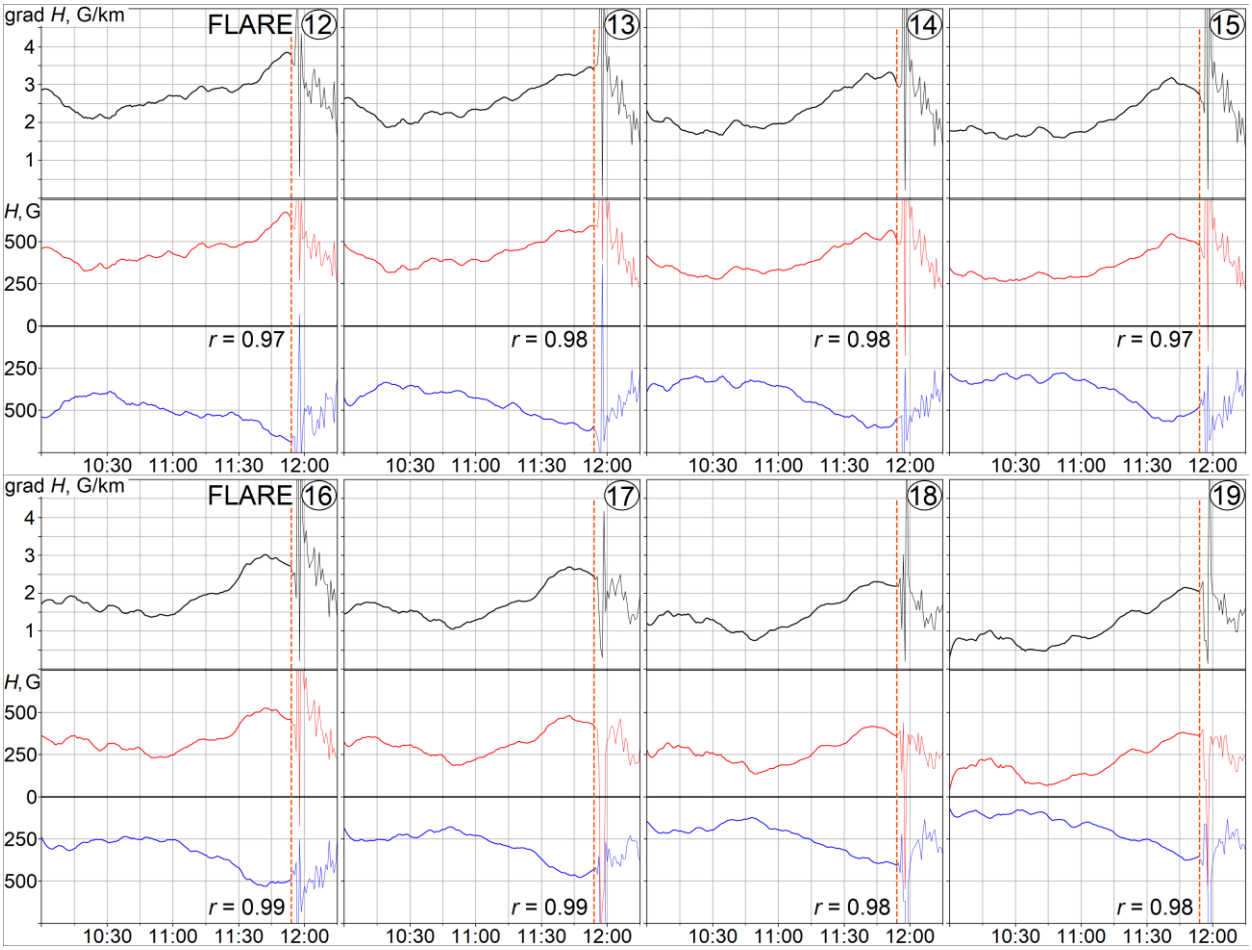

Figure 16. Variation in the magnetic field gradient in sections 12–19 of the main PIL before a powerful solar flare

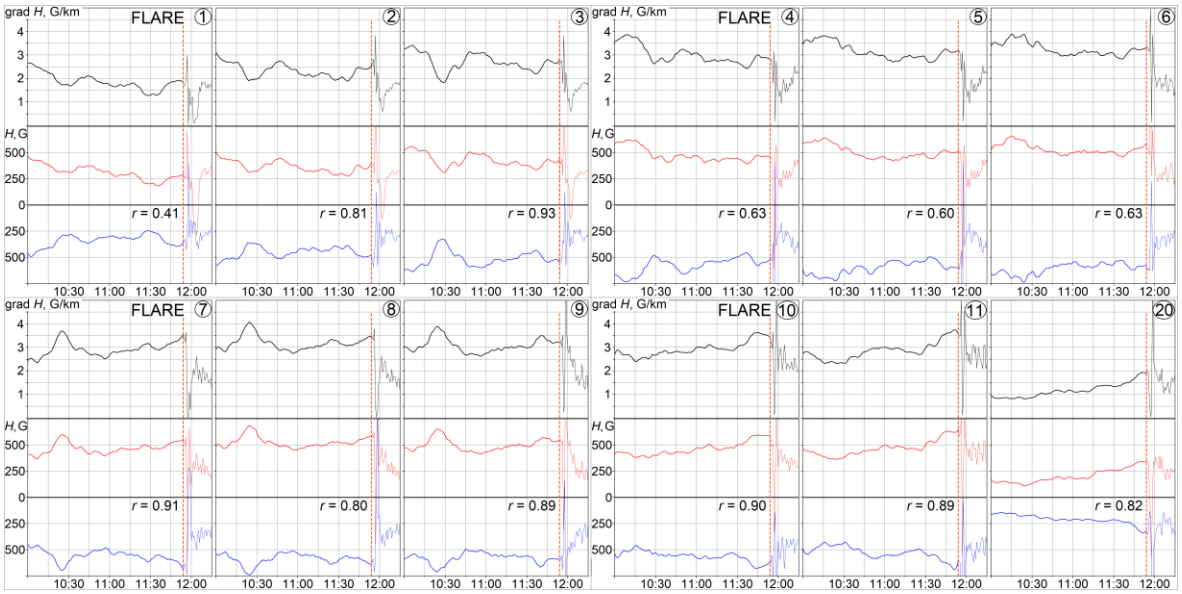

Figure 17. Variation in the magnetic field gradient in sections 1–11 and 20 of the main PIL before the September 06, 2017 powerful flare

The work was financially supported by Basic Research Program II.16.

REFERENCES

Altyntsev A.T., Banin V.G., Kuklin G.V., Tomozov V.M. *Solar Flares*. Moscow, Nauka Publ., 1982, 246 p.

Borovik A.V. Centers of flare activity of sunspot groups. Research on geomagnetism, aeronomy and solar physics. 1994, Vol. 102, pp. 133–152.

Borovik A.V. Low-power solar flares in the H_α line: research results. *Izvestiya Krymskoi Astrofizichesko. Observatorii*. 2023, vol. 119, no. 1, pp. 27–41.

Borovik A.V., Zhdanov A.A. Distribution of low-power solar flares by brightness rise time. *Solar-Terr. Phys*. 2018, vol. 4, no. 3, pp. 3–12. DOI: 10.12737/stp-43201801.

Borovik A.V., Zhdanov A.A. Low-power solar flares of optical and X-ray wavelengths for solar cycles 21–24. *Solar-Terr. Phys*. 2020, vol. 6, no. 3, pp. 16–22. DOI: 10.12737/stp-63202002.

Borovik A.V., Mordvinov A.V., Golubeva E.M., Zhdanov A.A. Restructuring of the solar magnetic fields and flare activity centers in cycle 24. *Astronomy Rep*. 2020, vol. 64, no. 6, pp. 540–546. DOI: 10.31857/S0004629920070014.

Cao T., Hu F., Xie G. Morphological properties of major spotless two-ribbon flare on 23 April 1981. *Scientia Sinica, Ser. A. Mathematical, Physical, Astronomical and Technical Sci*. 1983, vol. 26, pp. 972–977.

Hagyard M.J., Moore R.L., Emslie A.G. The role of magnetic field shear in solar flares. *Adv. Space Res*. 1984, vol. 4, no. 7, pp. 71–80. DOI: 10.1016/0273-1177(84)90162-5.

Heyvaerts J., Priest E.R., Rust D.M. An emerging flux model for the solar flare phenomenon. *Astrophys. J*. 1977, vol. 53, no. 1, pp. 255–258. DOI: 10.1086/155453.

Hoyng P., Duijveman A., Machado M.E., et al. Origin and location of the hard X-ray emission in a two-ribbon flare. *Astrophys. J*. 1981, vol. 246, no. 2,pp. LI55–LI59. DOI: 10.1086/183574.

Krivsky L. Interaction of magnetic fields and the origin of proton flare. *Proc. IAU Symposium. Structure and Development of Solar Active Regions*. 1968, no. 35, pp. 465–470.

McKenzie D.E. Signatures of reconnection in eruptive flares. *Yohkoh 10th anniversary meeting, COSPAR Colloquia Ser*. 2002, vol. 13, pp. 155–164. DOI: 10.1016/S0964-2749(02)80041-5.

Parker E.N. Nanoflares and the solar X-ray corona. *Astrophys. J*. 1988, vol. 330, pp. 474–479. DOI: 10.1086/166485.

Piddington J.H. Solar magnetic fields and convection. I. Active regions and sunspots. *Astrophys. Space Sci*. 1975, vol. 34, no. 2, pp. 347–362. DOI: 10.1007/BF00644803.

Priest E. *Solar Magnetohydrodynamics*. Moscow, Mir Publ., 1985, 592 p. (In Russian).

Romano P., Elmhamdi A., Kordi A.S. Two strong white-light solar flares in AR NOAA 12673 as potential clues for stellar superflares. *Solar Phys*. 2019, vol. 294, no. 4, pp. 4–8. DOI: 10.48550/arXiv.1812.04581.

Sundara R.K. Selvendran R., Thiagarajan R. On the triggering of quiet region flares without filament activation. *Bull. Astr. Soc. India*. 1997, vol. 25, pp. 533–540.

Svestka Z. *Solar flares*. Dordrecht: Reidel. 1976, 399 p.

Verma M. The origin of two X-class flares in active region NOAA 12673. Shear flows and head-on collision of new and preexisting flux. *Astron. Astrophys*. 2018, vol. 612, article number A101, p. 7. DOI: 10.1051/0004-6361/201732214.

Yang S., Zhang J., Zhu X., Song Q. Block-induced complex structures building the flare-productive solar active region 12673. *Astrophys. J. Lett*. 2017, vol. 849, L21, pp. 1–7. DOI: 10.3847/2041-8213/aa9476.

URL: http://jsoc.stanford.edu (accessed November 19, 2023).

URL: https://gong.nso.edu (accessed November 19, 2023).

Original Russian version: Borovik A.V., Zhdanov A.A., published in Solnechno-zemnaya fizika. 2023. Vol. 9. Iss. 4. P. 44–53. DOI: 10.12737/szf-94202305. © 2023 INFRA-M Academic Publishing House (Nauchno-Izdatelskii Tsentr INFRA-M)

How to cite this article

Borovik A.V., Zhdanov A.A. Dynamics of small-scale magnetic fields before small and large solar flares. *Solar-Terrestrial Physics*. 2023. Vol. 9. Iss. 4. P. 37–45. DOI: 10.12737/stp-94202305.